Oxidation of the N-terminal domain of the wheat metallothionein Ec-1 leads to the formation of three distinct disulfide bridges

Tarasava, Katsiaryna ; Chesnov, Serge ; Freisinger, Eva

DOI: https://doi.org/10.1002/bip.22849

Oxidation of the N-Terminal Domain of the Wheat Metallothionein E_c-1 Leads to the Formation of Three Distinct Disulfide Bridges

Journal:	*Biopolymers: Peptide Science*
Manuscript ID	BIP-PEP-2015-00056.R1
Wiley - Manuscript type:	Original Article
Date Submitted by the Author:	n/a
Complete List of Authors:	Tarasava, Katsiaryna; University of Zurich, Department of Chemistry Chesnov, Serge; University of Zurich/ETH Zurich, Functional Genomics Center Zurich Freisinger, Eva; University of Zurich, Department of Chemistry
Keywords:	metallothioneins, oxidation, disulfide bridges, MS/MS, proteolysis

Oxidation of the N-Terminal Domain of the Wheat Metallothionein E_c-1 Leads to the Formation of Three Distinct Disulfide Bridges

Katsiaryna Tarasava,[a] Serge Chesnov,[b] Eva Freisinger*,[a]

[a] *University of Zurich, Department of Chemistry, Winterthurerstrasse 190, 8057 Zurich, Switzerland*

[b] *University of Zurich/ETH Zurich, Functional Genomics Center Zurich, Winterthurerstrasse 190, 8057 Zurich, Switzerland*

Email: freisinger@chem.uzh.ch

ABSTRACT

Metallothioneins (MTs) are low molecular weight proteins, characterized by a high cysteine content and the ability to coordinate large amounts of d^{10} metal ions, e.g. Zn(II), Cd(II), and Cu(I), in form of metal-thiolate clusters. Depending on intracellular conditions such as redox potential or metal ion concentrations, MTs can occur in various states ranging from the fully metal-loaded holo- to the metal-free apo-form. The Cys thiolate groups in the apo-form can be either reduced or be involved in disulfide bridges.

Although oxidation-mediated Zn(II) release might be a possible mechanism for the regulation of Zn(II) availability by MTs, no concise information regarding the associated pathways and the structure of oxidized apo-MT forms is available. Using the well-studied $Zn_2\gamma$-E_c-1 domain of the wheat Zn_6E_c-1 MT we attempt here to answer several question regarding the structure and biophysical properties of oxidized MT forms, such as: (1) does disulfide bond formation increases the stability against proteolysis, (2) is the overall peptide backbone fold similar for the holo- and the oxidized apo-MT form, and (3) are disulfide bridges specifically or randomly formed?

Our investigations show that oxidation leads to three distinct disulfide bridges independently of the applied oxidation conditions and of the initial species used for oxidation, i.e., the apo- or the holo-form. In addition, the oxidized apo-form is as stable against proteolysis as $Zn_2\gamma$-E_c-1, rendering the currently assumed degradation of oxidized MTs unlikely and suggesting a role of the oxidation process for the extension of protein lifetime in absence of sufficient amounts of metal ions.

Keywords

metallothioneins; oxidation; disulfide bridges; MS/MS; proteolysis

INTRODUCTION

Metallothioneins (MTs) are a class of small (up to 12 kDa) intracellular proteins widespread in all phyla of life. Their name is derived from the high content of cysteine residues in their primary amino acid sequences, which can reach up to 30% in the mammalian forms, and the associated large binding capacity for metal ions, mainly with d^{10} electron configuration. The metal ions are coordinated if form of metal-thiolate clusters and determine the function of MTs in essential metal ion metabolism of, depending on the organism, Zn^{II} or Cu^{I} and in the detoxification of excess essential and also toxic non-essential metal ions such as Hg^{II} and Cd^{II}.[1-4] The cysteine thiolate groups have been also proposed to contribute to the protection against oxidative stress due to their high reactivity towards reactive oxygen (ROS) and nitrogen (RNS) species.[5] It was shown that MTs are capable to react 300 times faster with hydroxyl radicals than reduced glutathione (GSH) and that expression of some MTs is up-regulated by H_2O_2, in this way protecting against DNA strand cleavage by OH•.[6] The concomitant oxidation of the MT results in disulfide bridge formation. Generally, disulfide bridges in proteins can be formed via two mechanisms:[7,8] Thiol-disulfide exchange reactions represent a one-electron oxidation and are observed, for example, during the oxidation of Cys thiolates with glutathione disulfide (GSSG). The second possibility involves the formation of a sulfenic acid intermediate, which is formally a two-electron oxidation of the involved sulfur atom and has been detected upon oxidation of Cys residues with oxygen or H_2O_2. The sulfenic acid intermediate is usually rather short lived and reacts rapidly with other Cys thiolate groups in the vicinity to form a disulfide bridge.

Depending on the intracellular conditions such as redox potential and concentration of metal ions a given MT can adopt different states ranging from the fully metal-loaded and reduced holo-form to the metal-free apo-form, sometimes also denoted thionein (Figure 1). Fluorescent labeling of thiol groups in rat kidney and brain homogenates revealed that approximately 50% of the MTs present are in the apo-form. The value for rat liver is 27%.[9] Such apo-forms have been suggested to be important for the buffering of the intracellular free Zn^{II} ion

concentration.[10] While MTs exist in their apo-forms directly after ribosomal synthesis and prior to post-translational metal ion-loading, the metal-free form can be also formed in the cell by demetalation, either via competition with other enzymes, e.g. zinc fingers,[11,12] or chelators,[13] or via oxidation by ROS and RNS (Figure 1).[14] For rat liver (see above) it has been shown that actually one quarter of the apo-MT content is present in its oxidized state, i.e. 7% of the total MT content.[15]

>>> insert Figure 1 here <<<

Since the discovery of MTs, the main research focus has been on the biophysical and structural characterization of the holo-forms. Coordination of metal ions and formation of metal-thiolate clusters is assumed to be the critical factor for a defined three-dimensional structural fold as the unstructured peptide backbone wraps around the metal core.[16,17] In absence of metal ions, reduced apo-MTs generally do not adopt compact structures and exist as a highly dynamic and flexible polypeptide chains. However, the extend of this absence of three-dimensional structure is still under discussion. Support for the existence of unstructured peptide chains was obtained by NMR and circular dichroism (CD) spectroscopy. The NMR spectra of reduced apo-γ-E_c-1 (Figure S1, Supporting Information) show that all amide proton chemical shifts are located around 8-8.5 ppm, the region characteristic for random coil.[18] CD spectra of a number of apo-MTs reveal only one negative ellipticity band at 210 nm that originates from the natural chirality of amino acid residues in unfolded proteins.[22, 23] Nevertheless, it cannot be entirely excluded that the CD signals indicative for secondary structural elements were not detected due to low ellipticity values or because of signal overlap with other transitions.[24, 25] The presence of β-sheet structures was proposed for MTs that contain longer Cys-free amino acid stretches such as the plant MT1, MT2, and MT3 forms based on analyses with CD and IR spectroscopy.[19] In particular, these β-sheet structures were retained even in the metal-free state. Such a preservation of structural features was also derived for the recombinant human MT-1a form upon partial and even complete removal of coordinated zinc ions based on molecular dynamics simulations and on the ionization pattern obtained by mass spectrometry and explained by stabilization through a hydrogen bond network.[20] Hence taken together, there seems to be as much experimental evidence supporting the presence of structural features of some kind in apo-MT forms as there

are studies contradicting them. Nevertheless, it remains difficult to conceive that the observed unique and defined multidomain cluster structures, involving 20 Cys residues in the mammalian MTs, can be shaped starting solely from a random coiled peptide without any structural prefold. However, not only the folding process in presence of metal ions is of interest. Also the process and outcome of apo-MT oxidation is mostly unknown. A major open question is if oxidation results in a single defined structure with specifically formed disulfide bridges or if multiple oxidized structures with random disulfide bridge pattern are obtained. On the one hand, oxidation of an MT with a random coil structure is unlikely to produce a specific cystine connectivity pattern, except that disulfide bridges might be formed preferentially between Cys residues close in sequence to each other. On the other hand, a pre-folded apo-MT structure should provide a suitable scaffold for specific disulfide bridge linkages. The latter hypothesis was challenged by the following experiment. The β-domain of mouse Cd_7MT, i.e. Cd_3β-MT1, which forms a well-defined structure, was oxidized with NO and a NMR spectrum recorded.[21] As this spectrum did not reveal any signals, random disulfide bridge formation was concluded. Hence the lack of evidence for a distinct oxidized structure was taken as proof for the presence of a random structure in this case. Specific disulfide bridges were so far only described to occur intermolecularly in MT dimers, e.g. upon gradual oxidation of mouse Cd_7MT-1 at aerobic conditions[22] or in marine mussel MT1 after exposure to cadmium.[23,24]

To analyze the disulfide bridge formation process upon oxidation in more detail, we chose the γ-domain of the wheat E_c-1 MT as a target. This plant MT shows high expression levels in germ cells during embryogenesis and is assumed to play a role in Zn^{II} homeostasis.[25] The holo-form of wheat E_c-1, Zn_6E_c-1, folds into two domains, the N-terminal Zn_2γ-E_c-1 and the C-terminal $Zn_4\beta_E$-E_c-1 domain, containing 6 and 11 Cys residues, respectively.[26-28] The 26 amino acids long γ-domain peptide is especially suited for this study as it features the smallest divalent metal-thiolate cluster possible, i.e. Zn_2Cys_6, and because the three-dimensional structure of the Zn_2γ-E_c-1 form has been previously determined with solution NMR.[26] A special focus will be set on the following questions: (1) does formation of disulfide bonds increase the stability against chemical treatment and proteolysis, (2) is the overall fold of the peptide backbone similar in the metal cluster-containing holo- and the oxidized apo-MT form, and (3) does oxidation lead to specific or random formation of disulfide bridges?

RESULTS

Analysis of condition for the oxidation of apo- and $Zn_2\gamma$-E_c-1

Oxidation of MTs results in the formation of disulfide bridges and hence is accompanied by metal ion release from the metal clusters. For *in vitro* studies, several oxidation agents can be used, which differ in oxidation potential and either stimulate or not disulfide exchange during the oxidation process, denoted as disulfide scrambling. The most frequently used oxidants for this purpose are nitric acid,[21] hydrogen peroxide in presence or absence of Fe^{2+},[29] xanthine oxidase,[29] 5,5'-dithiobis(2-nitrobenzoic acid) (DTNB),[30,31] and glutathione disulfide (GSSG).[32] For the current study we selected two different oxidation agents. Hydrogen peroxide was chosen due to its large reduction potential of $E^{0'}$ = 1.343 V (pH 7, 25°C) and hence high oxidation power, its stability, specificity towards oxidation of only cysteine and methionine, but not of any other amino acids,[33] low absorptivity above 210 nm (Figure S2, Supporting Information), and its compatibility with the 2-PDS assay as well as with analysis by mass spectrometry. In addition, a GSH/GSSG mixture was used, which has a reduction potential that is closely similar to the one of the cysteine/cystine redox couple, i.e. $E^{0'}$ = –0.24 V *versus* $E^{0'}$ = –0.22 V (pH 7, 25°C).[34] On the one hand, the GSH/GSSG redox couple has biological relevance as it is the main regulation system for the intracellular redox potential. On the other hand, the similarity of the redox potentials and the possibility to form intermediate mixed disulfides (between oxidized MT thiolates and oxidized glutathione) allows progression of thiol-disulfide exchange reactions during the oxidation process and hence might promote formation of the thermodynamically most favored disulfide-bridge arrangement.[35] Equimolar mixtures (typically 2 mM each) of GSH and GSSG are often used for folding of Cys-rich proteins that contain high amounts of disulfide bridges in their native structures that need to be specifically formed for proper protein function. An example is the oxidative folding of cyclotides *in vitro*.[36] For the present study the use of a GSH/GSSG mixture is limited to certain experiments due to several experimental drawbacks, i.e. GSH is not compatible with the 2-PDS assay that is used to determine the concentration of reduced Cys thiol groups, γ-E_c-1 and GSSG cannot be separated by SEC due to overlapping elution volumes, and the affinity of GSH for Zn^{II} ions excludes its use in the metal ion competition experiments involving γ-E_c-1 and zincon.

Incubation of apo- or $Zn_2\gamma$-E_c-1 in 2 mM H_2O_2 for 8 h leads to complete oxidation according to the 2-PDS assay (Table S3, Supporting Information) and mass spectrometry (Figure S3, Supporting Information). The MS data shows only one major species with a molecular weight of 2454.8 Da corresponding to the oxidized apo-form with all six Cys residues involved in intramolecular disulfide bridges ($M_{r,calc}$ = 2454.9 Da for oxidized and $M_{r,calc}$ = 2461.0 Da for reduced apo-γ-E_c-1). Only minor signals for species with higher sulfur oxidation states were detected such as sulfenic (–SOH), sulfinic ($–SO_2H$), or sulfonic acids ($–SO_3H$).[37] Size exclusion chromatography (SEC) of oxidized apo-γ-E_c-1 gives a major elution peak corresponding to the monomeric protein and only small amounts of γ-E_c-1 multimers were formed, most probably via intermolecular disulfide bridges (Figure S4, Supporting Information).

Also incubation of apo-γ-E_c-1 with a 2 mM GSH/GSSG mixture for 8 h under strictly anaerobic conditions results in completely oxidized apo-γ-E_c-1 according to the peak assignment after SEC and analysis with the 2-PDS assay (Figure S5, Supporting Information, Table S1, Supporting Information). In contrast, oxidation of $Zn_2\gamma$-E_c-1 is incomplete under these conditions and one equivalent of Zn(II) is retained (Table S1, Supporting Information). Analysis of this sample with MS was performed at neutral pH to preserve metal ion binding, and mass peaks corresponding to Zn_2-, Zn_1-, as well as oxidized apo-γ-E_c-1 were observed (Figure S6A, Supporting Information). At acidic pH, and hence after metal ion release, mass data with isotopic resolution of the species can be collected and show signals originating from the reduced form as well as from species with one and two disulfide bridges. In addition, very low intensity mass peaks for the completely oxidized form with three disulfide bridges are observed (Figure S6B, Supporting Information). Note that these MS analyses are qualitative in nature and are not a reliable measure for species quantification. The partially oxidized $Zn_1\gamma$-E_c-1 species will be discussed further and in more detail below (see 'Assignment of disulfide bridge connectivities with tandem MS/MS'). The summary of all oxidation conditions used and the resulting species are depicted in Figure 2.

>>> insert Figure 2 here <<<

Oxidation of $Zn_2\gamma$-E_c-1 and Zn^{II} release followed by UV and CD spectroscopy

The UV spectra of holo-MTs are dominated by the respective ligand-to-metal charge transfer (LMCT) bands centered, e.g., at 230 nm for thiolate-Zn(II) and at 250 nm for thiolate-Cd(II) transitions with molar extinction values in the range of roughly 4500-5000 M^{-1} cm^{-1} per Zn-S or Cd-S transition. In contrast, the molar extinction of disulfide bonds is only weak, e.g. the spectrum of cystine (Figure S8, Supporting Information) shows a pH-independent band around 245 nm with a molar absorptivity of approximately 360±10 M^{-1} cm^{-1} that tails up to 300 nm (ε_{280nm} 124±10 M^{-1} cm^{-1}).[38,39] Accordingly, the transitions of disulfide bonds can be masked by the LMCT bands of Zn^{II}- and Cd^{II}-thioneins or theoretically also by transitions of aromatic amino acids. However, as the γ-E_c-1 domain, in contrast to most other plant MTs, is devoid of aromatic amino acids, the absorption at 280 nm can be used here to monitor disulfide bridge formation, which is another advantage of the chosen system. For the analysis of metal ion release and oxidation a 10 μM $Zn_2\gamma$-E_c-1 solution was incubated with 2 mM H_2O_2 and spectra were recorded in the time range 0-350 min (Figure 3). A GSH/GSSG mixture cannot be used as oxidant in this experiment due to its absorption in the relevant spectral range and its interaction with Zn(II) ions.

>>> insert Figure 3 here <<<

The decrease of the LMCT band at 230 nm and the absorptivity increase of transitions originating from the disulfide bridges in the broad range of 255-310 nm clearly show the release of Zn(II) ions and the concomitant oxidation of the protein, which is complete after approximately 160 min (Figure 3B). While Zn(II) release follows an almost linear time-dependence and 50% Zn(II) release is observed after 50 min, the formation of disulfide bridges shows a rather long lag-phase and only sets on at this time point (Figure 3C). This observation fits to a hypothetical Zn_1-species in which the two non-coordinating cysteine sulfur atoms are in an oxidation state different from the –I oxidation state in a disulfide bridge (denoted with * in Figure 3C, species I) and hence do not absorb in the 255-310 nm wavelength range. One explanation would be the formation of cysteine sulfenic acid intermediates that subsequently comproportionate with cysteine thiol groups to disulfide bridges.[40,41] It is also possible, that one or both of the Cys sulfur atoms are still reduced. Reduced Cys thiolates contribute to the absorption at 230 nm but only with roughly 10% of the absorptivity of thiolate-Zn(II) transitions.

75% Zn^{II} release is reached after approximately 90 min, which is in agreement with a 1:1 mixture of Zn_1- (I) and apo-γ-E_c-1 species. As the ε_{280nm} value at 90 min indicates on average the presence of 1-1.5 disulfide bridges (taking into account the low molar extinction value of disulfide bridges and hence the greater error range of the values), different mixtures of species are possible, for example a 1:1 mixture of species I and II or of I and III. Finally, after complete Zn^{II} release also the maximum absorptivity value for the disulfide bridges is reached and hence a completely oxidized apo-γ-E_c-1 species (III) is obtained.

In an alternative approach, the Zn(II) release in presence of 2 mM H_2O_2 was monitored with the Zn(II)-chelator zincon. The Zn(II)-zincon complex has a characteristic absorption at 620 nm with an extinction coefficient ε_{620nm} of 19'450 M^{-1} cm^{-1} under the experimental conditions applied (literature value 17'500 M^{-1} cm^{-1}).[42] Interestingly, Zn(II) release in presence of zincon is much slower (350 min compared to 160 min, Figure 4A) than without this chelator, the reason for this not being clear.

Both experiments allow the calculation of the first order rate constant of Zn(II) release from the γ-E_c-1 domain using the following equation:[32,43]

$$\ln \frac{A_{start} - A_t}{A_{start} - A_{end}} = k \cdot t \qquad \text{(Eq. 1)}$$

The respective plot of $\ln((A_{start}-A_t)/(A_{start}-A_{end}))$ against the incubation time is depicted in Figure 4B for the experiment with zincon, and rate constants for four different time ranges corresponding to the release of 25, 50, 75, and 100% Zn(II) are given in the figure legend as well as an average constant (k_{av}) for the entire range. Each of the four constants is twice as large in the experiment without the chelator (Figure 3C; Figure S9, Supporting Information) and hence the entire process is slowed down in the presence of zincon and not just a just part of it. A very similar value of $(2.88 \pm 0.02) \times 10^{-4}$ s^{-1} is obtained when Zn_2E_c-1 is incubated with a mixture of 1 mM GSH and 4.5 mM GSSG and metal ion release is quantified with the Zn(II)-chelator 4-(2-pyridylazo)resorcin (PAR).[32]

>>> insert Figure 4 here <<<

Another method to follow the oxidation process is based on changes of the protein structure than can be monitored by CD spectroscopy. Generally, the far-UV range of protein CD spectra

up to 240 nm is dominated by the peptide bond as chromophore and hence this region is indicative for secondary structures such as α-helix and β-sheet but also for random coil structures that prevail in MTs. Bands in the near-UV range of 260-320 nm show usually far less than 1% of the ellipticity values observed for the bands in the far-UV region and originate from aromatic amino acids. Additional contributions in this range can arise from disulfide bridges resulting in a very broad and weak signal centered around 260 nm.[44] Most MTs, including the wheat E_c-1 protein, are devoid of aromatic amino acids, however, in this protein class the metal-thiolate clusters can act as additional chromophores. Typically, the corresponding CD bands are observed in the broad wavelength range around the position of the respective LMCT bands in the UV/Vis spectra, i.e. around 230 nm for Zn(II) and around 250 nm for Cd(II)-MTs.[45,46] Figure 5 depicts the spectra of reduced apo- as well as $Zn_2\gamma$-E_c-1, and the differences arising from the overlapping contributions of the peptide backbone structure and the Zn_2Cys_6 cluster are clearly visible in the range of roughly 210-250 nm. Upon oxidation, the maxima at 250 and 225 nm in the spectrum of $Zn_2\gamma$-E_c-1 that are attributed to the cluster disappear as expected. Oxidation of the apo-form leads to an ellipticity increase in the far-UV region and can be explained with decreased peptide backbone flexibility upon disulfide bridge formation. However, transitions below 210 nm in these measurements (grey box in Figure 5) are to be interpreted with caution due to saturation of the detector at the concentrations used. After 3 h identical spectra are obtained regardless if oxidation of apo- or $Zn_2\gamma$-E_c-1 was performed, corroborating formation of identical completely oxidized, metal-free forms under both conditions.

>>> insert Figure 5 here <<<

Reduction of oxidized γ-E_c-1

Mild oxidation of cysteines to the oxidation state –I as occurring in disulfide bridges is a reversible process *in vivo*. In plant cells reduction is achieved by the glutathione/glutaredoxin or the thioredoxin/thioredoxin reductase system and by the GSH/GSSG redox couple.[47-50] In the absence of oxidative stress, GSH concentrations are generally distinctively higher than the GSSG concentrations ranging between 2-4 mM.[51] Hence, for the reduction experiments of oxidized γ-E_c-1 an intermediate concentration of 3 mM GSH was used. The oxidized γ-E_c-1 species were obtained in four different ways as described above:

sample 1: $Zn_2\gamma$-E_c-1 + 2 mM H_2O_2

sample 2: reduced apo-γ-E_c-1 + 2 mM H_2O_2

sample 3: reduced apo-γ-E_c-1 + 2 mM GSH/GSSG

sample 4: $Zn_2\gamma$-E_c-1 + 2 mM GSH/GSSG

As stated above, analyses after dialysis show that samples 1-3 are completely oxidized (Table S1, S3, Supporting Information), while sample 4 still contains one equivalent of Zn(II) and is only partially oxidized according to the PDS assay (Figure S5 Peak 1, Tables S1 and S3, Supporting Information) and MS measurements (Figure S6A, Supporting Information). Samples 1-3 remained completely oxidized after 5 h of incubation with 3 mM GSH (Table S3, Supporting Information). For sample 4 a certain degree of reduction was observed in the MS spectra (Figure S10, Supporting Information). While the MS spectrum before reduction reveals a mixture of fully reduced apo-γ-E_c-1, species containing one or two intramolecular disulfide bridges and even low intensity signals for a species containing three disulfide bridges, the highest intensity signals after reduction originate from the fully reduced apo-γ-E_c-1 form and only low intensity signals for the species with one and two disulfide bridges are observed. A possible explanation, why only partially oxidized γ-E_c-1 can be re-reduced, might be the sterically restricted accessibility of cystines by the reductant in a compact oxidized structure. Further experiments with enzymatic reduction systems might provide more insight into the reduction process.

Assignment of disulfide bridge connectivities with tandem MS/MS

Analysis of fully oxidized γ-E_c-1

The distribution pattern of the Cys residues in the γ-E_c-1 domain has a certain similarity to the one observed in cyclotides. Cyclotides are a class of small backbone cyclized proteins found mainly in plants that contain usually six Cys residues engaged in three disulfide bridges forming a motive denoted as cyclic cystine knot. The most well-known member of the cyclotide family is the kalata B1 protein.[52] The amino acid alignment of the γ-E_c-1 sequence with a smaller cyclotide, the 34 amino acids long MCoTI-II protein from *Momordica cochinchinensis* is shown in Figure 6A and reveals even a certain sequence similarity.[53] Upon oxidation, also the six Cys residues of the γ-E_c-1 domain form three intramolecular disulfide bridges as discussed above (Figure S3, Supporting Information).

To identify the disulfide-linked residues, the peptide fragments obtained after tryptic digestion of a fully oxidized γ-E_c-1 form were analyzed by tandem MS/MS spectrometry (a detailed evaluation can be found in the Supporting Information including Figures S11-S13, as well as Tables S4 and S5). The data show formation of exactly three specific intramolecular disulfide bridges (Figure 6B, C). While covalent bonds between residues Cys8 and Cys10 as well as Cys14 and Cys20 are unambiguously identified in multiple fragment ions, proof for the disulfide bridge involving Cys4 and Cys22 is limited due to its special position within the structure. Only one fragment ion, assigned to the disulfide bridged peptide fragments Gly1-Asp6 and Cys22-Arg26 (found 1069.1 Da; calc. 1069.4 Da), can directly support this connectivity. Rather surprisingly, the same specific disulfide bridge pattern is observed when the reduced apo-γ-E_c-1 form was used as starting compound for complete oxidation with H_2O_2 (Figures S14-S16, Supporting Information).

>>> insert Figure 6 here <<<

Analysis of partially oxidized Zn_1γ-E_c-1

In addition to the study with the fully oxidized apo-γ-E_c-1 domain, also the disulfide bridge pattern in the partially oxidized sample of the general composition Zn_1γ-E_c-1 was investigated. This stoichiometry seems to represent a rather stable intermediate in the oxidation process as it can be obtained from Zn_2γ-E_c-1 upon incubation with a 2 mM GSH/GSSG mixture for 8 h (Figure S6, Supporting Information, Table S1, S3, Supporting Information). For the analysis of the intermediate oxidation product(s) by MS, the partially oxidized Zn_1γ-E_c-1 sample was prepared using 1.5 mM H_2O_2, because this oxidant, in contrast to a GSH/GSSG mixture, does not interfere with the measurement. To monitor and validate the correct stoichiometry of the partially oxidized sample, small amounts of the reaction mixture were taken at different time points during the oxidation process. The metal ion content of each sample was analyzed with F-AAS after incubation with Chelex® 100 resin, while the –SH content was directly determined with the 2-PDS assay, which is not influenced by H_2O_2 under the conditions used here (Table S6, Supporting Information). After 50 min of incubation a sample containing approximately 1.2 equiv of Zn^{II} and 4.7 reduced Cys residues per MT molecule was obtained. This sample was alkylated with iodoacetamide (IAA) to prevent further Cys oxidation during MS sample

preparation and analysis. In addition, the introduced acetamide groups can serve as "labels" to identify non-oxidized Cys residues in the spectra. The deconvoluted ESI-MS data (Figure S17, Supporting Information) shows species with zero, two, four, and even six modified Cys residues corresponding to a mixture of completely oxidized apo-γ-E_c-1, partially oxidized species with two and one disulfide bridge, as well as the completely reduced form. Subsequently, the mixture was digested with trypsin and analyzed by MALDI-MS/MS following the same procedure as for the fully oxidized apo-γ-E_c-1 form described above and in the Supplementary Information.

Already the MS data of the tryptic digest (Figure S18, Supporting Information) give some indications about the possible Cys connectivity pattern. The peptide fragment Cys8-Arg21 that contains four Cys residues occurs both fully reduced and with one disulfide bridge (1508.6 and 1392.5 Da). MS/MS data show distinctive fragment ions that support a linkage between Cys14 and Cys20 and acetamide modified Cys8 and Cys10 residues (Figure 7, species Ib). In addition, lower intensity fragment ions corroborate a second species with a Cys8-Cys10 linkage as well as modified Cys14 and Cys20 residues (Figure 7, Ic; Figure S19, Supporting Information, Table S7, Supporting Information).

Another mass can be assigned to the linked peptide fragments Cys8-Arg21 and Cys22-Arg26 including one modified and hence reduced Cys residue (1869.7 Da; Figure S18, Supporting Information). The MS/MS data again clearly reveal the presence of a disulfide bridge between Cys14 and Cys20 (Figure S20, Supporting Information; Table S8, Supporting Information). If Cys22 is linked to Cys8 or Cys10 cannot be decided (Figure 7, IIb) as no additional signals corroborating either of the two possibilities are observed.

The species at m/z 2111.7 (Figure S18, Supporting Information) originates from the peptide Gly1-Arg21 modified with three acetamide groups (calc. 2110.8 Da) and hence contains one intramolecular disulfide bridge. The MS/MS data (Figure S21, Supporting Information, Table S9, Supporting Information) corroborate a mixture of two species showing two different disulfide bridge connectivities, i.e. either between Cys4-Cys8 (Figure 7, Id) or between Cys14-Cys20 (Ia).

Two more tryptic digest fragments were analyzed by MS/MS: the ion at 1985.8 assigned to the peptide Cys8-Arg21 modified with three acetamide groups and linked to peptide Cys22-Arg26 and the ion at 1995.7 Da originating from peptide Gly1-Arg21 modified with one acetamide group (Figure S18, Supporting Information). Due to their similar masses, the two

peptide fragments had to be analyzed in the same measurement (Figure S22, Supporting Information, Table S10, Supporting Information), however, most fragment ions can be clearly distinguished. According to the MS/MS data, Cys14 and Cys20 in peptide Cys8-Arg21 are clearly reduced and accordingly the disulfide bridge to peptide Cys22-Arg26 must involve next to Cys22 either Cys8 or Cys10. However, only a single fragment ion unambiguously corroborates a linkage between Cys8 and Cys22 (Figure 7, Ie). Peptide Gly1-Arg21 contains two disulfide bridges, one of which is again formed between Cys14 and Cys20. For the second bridge, different fragment ions support either a linkage between Cys8 and Cys10 or between Cys4 and Cys8. Accordingly, there seems to be again a mixture of species differing in the second disulfide bridge (Figure 7, IIa).

Summarizing, partial oxidation of the $Zn_2\gamma$-E_c-1 form yields a mixture of species with zero, one, two and three disulfide bridges (Figure S17, Supporting Information). The species with two disulfide bridges (Figure 7, IIa,b) contain always one bridge between Cys14 and Cys20. The second bridge can be formed from Cys8 to Cys4, to Cys10, or to Cys22 or between Cys10 and Cys22. The species with one disulfide bridge (Figure 7, Ia-e) should all still possess the ability to coordinate one Zn(II) ion, but coordination of this Zn(II) ion is not restricted to a certain binding site. It should be noted, however, that partial oxidation of the protein most likely influences the binding site environments and hence metal binding abilities and affinities cannot be compared to the binding sites in the fully reduced protein. The single disulfide bridge is either formed between Cys14 and Cys20 (species Ia, Ib) or involving Cys8 with Cys4, Cys10, or Cys22 (Ic-e). In Ie also a bridge between Cys10 and Cys22 is feasible.

>>> insert Figure 7 here <<<

Stability against proteolytic digestion

The main cellular mechanisms for the removal of dysfunctional or redundant proteins is proteolysis. To analyze the stability of the different γ-E_c-1 forms against (limited) proteolytic digestion, the reduced and oxidized apo-forms as well as the $Zn_2\gamma$-E_c-1 form were incubated with proteinase K. Although this protease is not of plant origin, it is well-suited for a general comparison of the stabilities as the γ-E_c-1 domain contains an intermediate number of potential proteinase K cleavage sites (Figure 8A). In addition, the protease is rather stable and active at

physiological pH, which allows also the study of the Zn(II)-containing form under the same conditions. After digestion, the resulting mixtures were analyzed and purified by SEC in 10 mM ammonium acetate buffer, pH 7.5 (Figure 8C, D), and further analysed by mass spectrometry.

>>> insert Figure 8 here <<<

The size exclusion chromatograms show identical retention volumes of the $Zn_2\gamma$-E_c-1 form before and after digestion (Figure 8B). This alone does not exclude partial hydrolysis of the peptide backbone as cleaved peptide fragments could be still connected by the intact metal-thiolate cluster.[27,54] However, MS measurements performed at acidic pH (Figure S23, Supporting Information) solely reveal mass data for the full-length domain including species with cleaved C-terminal residues. In contrast, the backbone of the reduced apo-γ-E_c-1 form was cleaved in several positions and consequently the elution volume is shifted considerably towards volumes for smaller peptide fragments (Figure 8C). These two experiments, i.e. digestion of the folded metal-thiolate cluster containing form *versus* digestion of the presumably unfolded reduced apo-protein, demonstrate distinctly that the protein fold and hence the accessibility of cleavage sites have a strong influence on the cleavage efficiency and consequently on the stability of a given protein towards proteolytic digestion.

Analysis of oxidized apo-γ-E_c-1 with SEC reveals a larger elution volume than observed for the reduced apo- and Zn_2-forms suggesting a more compact structure. Nevertheless, deduction of a regular fold with NMR spectroscopy was, in contrast to studies with the $Zn_2\gamma$-E_c-1 form, not possible. The fragments observed by MS after digestion (Figure S23, Supporting Information) originate mainly from the non-cleaved full-length peptide with only some C-terminal amino acids cleaved as similarly observed for the metal-thiolate cluster containing form (Figure 8C). Hence the oxidized apo-form is distinctively more stable against proteolytic digestion than the reduced apo-form, and in this respect very similar to the holo-form.

DISCUSSION

The high Cys content of MTs is the prerequisite for the typical metal-thiolate cluster formation with d^{10} transition metal ions. While these clusters have a high thermodynamic stability, the low redox potential of the metal bound thiolate groups makes the ligands

susceptible to oxidation by rather mild oxidants and under oxidative stress conditions, a process that is accompanied by metal ion release and the formation of disulfide bridges.[40, 63-65] This oxidation sensitivity let to the proposal of a potential role of MTs in cellular redox buffering. Despite the fact that apparently up to 50% of the MT molecules within a cell can be present in the oxidized apo-state, very little is known about the structure and properties of apo-MTs. The purpose of this work was thus to perform a case study with the γ-E_c-1 domain, which hosts the smallest divalent metal-thiolate cluster feasible, i.e. Zn_2Cys_6, focusing on the structural aspects of the corresponding oxidized species.

Analysis of the partially oxidized Zn_1γ-E_c-1 sample neither shows a preferentially formed disulfide bridge nor the specific release of Zn(II) from one of the two binding sites. While the two disulfide bridges Cys8-Cys10 and Cys14-Cys20 were detected both in the partially oxidized Zn_1γ-E_c-1 sample as well as in the fully oxidized apo-form, also other connectivities involving Cys4, Cys8, Cys10, and Cys22 were observed in the partially oxidized sample and hence a certain rearrangement of the disulfide bridges must occur upon full oxidation. Overall, the analysis allows the general conclusion that the oxidation sensitivities of the six Cys residues are apparently quite similar.

In the fully oxidized γ-domain exclusive formation of exactly three distinct disulfide bridges is observed. This is surprising in light of the results with the partially oxidized protein and even more when considering that the same bridges were observed regardless if oxidation was performed with the Zn_2- or the reduced apo-form and independent of the oxidation agent used. To the best of our knowledge, this is the first example of such a high degree of specificity in disulfide bridge formation in a given MT. The observed disulfide bridge pattern can be reasonably explained for the prefolded Zn_2-form as all bridges are formed between Cys residues that were initially coordinating to the same metal ion and hence were close in space to each other before oxidation. This applies in particular to the bridge between Cys4 and Cys22, and hence between residues that are located at opposite ends of the amino acid sequence. Reduced apo-MTs are however generally viewed as intrinsically unstructured proteins and, while disulfide bridges between neighboring Cys residues, i.e. Cys8-Cys10 and Cys 14-Cys20, are easily perceivable, the observed Cys4-Cys22 bridge is highly unusual. One hypothesis could be that the preferred formation of the two disulfide bridges Cys8-Cys10 and Cys14-Cys20 (be it because there are rather close in sequence or because there are other attractive forces between residues in this area)

also brings the peptide ends close in space to enable formation of the third bridge between Cys4 and Cys22. Certainly the question remains, why Cys8-Cys10 and Cys14-Cys20 are specifically formed and no bridges between Cys4-Cys8, Cys10-Cys14 and/or Cys20-Cys22 are observed, which are also close to each other in the sequence. It can be further hypothesized that at least for the γ-E_c-1 domain, the correct three-dimensional fold might not strictly depend on metal ion coordination and hence metal-thiolate cluster formation. While the tetrahedral tetrathiolate coordination of Zn(II) ions leads to structural restraints between four Cys residues, each disulfide bridge connects just two Cys, and this might be already enough to allow the peptide chain to "find" its thermodynamic minimum for a folded structure in the folding landscape. Hence both, metal ion binding and oxidation, might both lead to the same overall structure, that is however more compact in the oxidized state due to the shorter SS bonds compared to Zn(II)-S bonds. Additional support for this view, i.e. that also less constraints can lead to the "correct" structure, comes from the observation that some MTs that preferentially coordinate divalent metal ions such as Zn(II) and Cd(II) are also able to coordinate isostoichiometric amounts of Cu(I) or Hg(II) ions that prefer tri- or only dithiolate coordination environments. In the resulting species a specific cluster structure is preserved according to the UV spectra that changes only upon addition of a metal ion excess.[19,55,56] Hence, it can be proposed that in these MTs the peptide structure is preserved to a certain extent although the more strict structural constraint of the tetrathiolate coordination was lost.

Considering the possible *in vivo* function and further fate of oxidized MT species it is worth to notice that the oxidized apo-γ-E_c-1 form seems to have a comparable stability against proteolysis as the metal loaded form, while reduced apo-γ-E_c-1 is rapidly digested. Hence it is reasonable to doubt the proposed cellular degradation of oxidized MTs and it should be rather assumed that oxidation might play a protective role leading to extended protein lifetimes. This view also moves a re-reduction mechanism of oxidized MTs into the realms of possibility.

Nevertheless, all experiments presented here were performed *in vitro*. Future studies should aim to elucidate the redox state of MTs *in vivo* in dependence of the cellular redox state or the presence of oxidizing agents in the growth media. Certainly, whenever possible it should be also considered that in living systems enzymatic isomerization of disulfide bridges as well as enzyme assisted oxidative protein folding can occur,[57] which could also not be taken into account in the present study.

The authors gratefully acknowledge Prof. em. Milan Vašák and Ms. Jelena Habjanic for helpful discussions. Financial support comes from the University of Zurich (Forschungskredit to KT), the Swiss National Science Foundation (EF), the Faculty of Natural Sciences, as well as the Department of Chemistry, University of Zurich.

MATERIALS AND METHODS

Chemicals and reagents

Tris(hydroxymethyl)aminomethane hydrochloride (Tris-HCl) and isopropyl β-D-thiogalactopyranoside (IPTG) were obtained from Biosolve (Chemie Brunschwig AG, Switzerland), Chelex® 100 resin from Bio-Rad (Switzerland), Luria-Bertani (LB) media used for *Escherichia coli* expression from Carl Roth AG (Switzerland), tris(2-carboxyethyl)phosphine (TCEP) from Fluorochem (Chemie Brunschwig AG), *Tritirachium album* proteinase K from Qbiogene (MP Biomedicals, Switzerland), trypsin from Roche Diagnostics (Mannheim, Germany), acetonitrile (ACN) from Merck (Switzerland), and reduced L-glutathione (GSH) from Carl Roth AG (Switzerland). All other reagents, including iodoacetamide (IAA), trifluoracetic acid (TFA), and the MALDI matrices α-cyano-4-hydroxycinamic acid (CHCA) and 2-(hydroxyphenylazo) benzoic acid (HBPA), were purchased in ACS grade from Sigma-Aldrich or Fluka (Switzerland).

Purification of the γ-E_c-1 domain

The wheat γ-E_c-1 domain was overexpressed in form of its GST-fusion protein and purified as previously described including removal of the GST-tag with thrombin.[26] Complete reduction of Cys residues was assured by treatment with 30 mM TCEP in 10 mM Tris-HCl buffer, pH 3, for 20 min followed by size-exclusion chromatography (SEC) in 10 mM HCl (HiLoad 16/600 Superdex 30 pg column, GE Healthcare). After quantification of thiol groups with 2,2′-dithiodipyridine (2-PDS assay)[58] the γ-E_c-1 domain was stored at -80 °C for future use. For all following procedures special care was taken to exclude any traces of oxygen. Accordingly, all solutions were degassed under vacuum and saturated with argon. Wherever possible, experiments were performed in a Type B Vinyl Anaerobic Chamber (Coy Lab, USA) equipped

with a palladium catalyst and operated with a 5% hydrogen/95% nitrogen gas mix. For the spectroscopic measurements septum-sealed cuvettes (Hellma AG, Switzerland) were used.

Preparation of fully oxidized γ-E_c-1

The pH of an oxygen-free solution of 30-50 μM completely reduced apo-γ-E_c-1 in 10 mM HCl was adjusted to 7.5 with ammonium acetate (10 mM final buffer concentration). Then, depending on the downstream experiment, either a GSH/GSSG mixture (2 mM final concentration each) or H_2O_2 (2 mM final) was added. After overnight incubation at room temperature low molecular weight components such as H_2O_2, GHS, GSSG, and Zn^{2+} ions were removed either by SEC for the samples containing GSH/GSSG or by dialysis for the samples containing just H_2O_2 as oxidant. Complete oxidation was verified with the 2-PDS assay.

For the oxidation experiments starting from the Zn_2γ-E_c-1 form, the fully metal ion-loaded peptide was prepared by addition of 2.1 equivalents of Zn(II) ions to reduced apo-γ-E_c-1 in 10 mM HCl followed by addition of ammonium acetate buffer (10 mM final) and pH adjustment with NaOH to 7.5. The Zn(II) excess was removed by dialysis against 10 mM ammonium acetate, pH 7.5, using a Tube-O-Dialyzer™ device with a molecular weight cut-off of 1 kDa (G-Biosciences, Socochim SA, Savigny, Switzerland). Oxidation was again performed overnight in two different ways: Either with 2 mM H_2O_2 followed by dialysis against 10 mM ammonium acetate, pH 7.5 (this sample was further used for MS analysis of the disulfide connectivity assignment), or with a 2 mM GSH/GSSG mixture followed by a SEC purification step (Superdex Peptide 10/300 GL column, GE HealthCare). The degree of Cys oxidation and Zn(II) release was determined with the 2-PDS assay and flame atomic absorption spectroscopy (F-AAS), respectively. While the sample obtained by oxidation with H_2O_2 is completely oxidized, oxidation with the GSH/GSSG mixture leads to a sample with a Zn(II):γ-E_c-1 stoichiometry of 1:1.

Zn(II) release under oxidative conditions

Zn(II)-release was studied in two different ways, either with UV spectroscopy based on the decreasing absorptivity of the thiolate-to-Zn(II) charge transfer band at 230 nm or by monitoring the increase of the absorptivity at 620 nm arising from the formed Zn(II)-zincon complex.

For the first experiment, a solution of 10 μM $Zn_2\gamma$-E_c-1 in 10 mM Tris-HCl, 10 mM NaCl, pH 7.5 was mixed with 2 mM (final concentration) H_2O_2 followed by immediate acquisition of UV spectra in the range 200-600 nm up to 350 min using a Cary 100 spectrophotometer (Agilent Technologies, Switzerland).

For the second experiment, 100 μM 2-carboxy-2-hydroxy-5-sulfoformazylbenzene (zincon) was added to a solution of 10 μM $Zn_2\gamma$-E_c-1 in 10 mM Tris-HCl, 10 mM NaCl, pH 7.5, and the mixture incubated with 2 mM (final concentration) H_2O_2. Zn(II) release was monitored at 620 nm up to 830 min using a Cary 100 spectrophotometer.

Proteinase K cleavage experiments

To compare the proteolytic stability of $Zn_2\gamma$-E_c-1, reduced apo-γ-E_c-1, and oxidized apo-γ-E_c-1, a 40 μM solution each was incubated with *T. album* proteinase K in a molar ratio of 5:1 for 30 min at 27 °C in a buffer containing 50 mM Tris-HCl, pH 8, and 10 mM $CaCl_2$. Subsequently, the mixture was analyzed and separated by SEC using a Superdex Peptide 10/300 GL column (GE Healthcare) in 10 mM ammonium acetate buffer, pH 7.5, and a flow rate of 0.5 ml min^{-1}. Fractions containing the γ-E_c-1 domain or its fragments were collected, combined, and analyzed by ESI-MS.

Reduction of (partially) oxidized γ-E_c-1 with GSH

Samples of the (partially) oxidized γ-E_c-1 domain were either prepared from apo- or $Zn_2\gamma$-E_c-1 using GSSH/GSH or H_2O_2 as oxidative reagents as described above and the released metal ions were removed by dialysis. From these four different preparations, only the one obtained from $Zn_2\gamma$-E_c-1 by oxidation with the GSH/GSSG mixture still contained one equivalent of Zn^{II}.
To analyze the reversibility of MT oxidation, 3 mM (final concentration) GSH was added to each of the four solutions of (partially) oxidized γ-E_c-1 and the mixtures were incubated for 5 h under strictly anaerobic conditions. Subsequent dialysis against 10 mM ammonium hydrogencarbonate, pH 7.5, was performed within the anaerobic chamber using vacuum degassed and argon saturated solutions. The total MT concentration in each sample was determined from its absorption at 205 nm with the Scopes method which uses an average extinction coefficient of 31 L g^{-1} cm^{-1} for a protein without tyrosine or tryptophan residues.[59] Multiplied by the molar mass of γ-E_c-1 (2461.7 g mol^{-1}) this results into ε_{205} = 76'312.7 M^{-1} cm^{-1}, which agrees well with the

value experimentally determined for a sample of oxidized γ-E_c-1 of known concentration, i.e. 76'315 M^{-1} cm^{-1}. The concentration of reduced –SH groups was again determined with the 2-PDS assay, and the concentration of remaining Zn(II) ions in the samples generated from Zn_2γ-E_c-1 was measured with F-AAS.

Circular dichroism measurements

CD spectra were measured on a Jasco J-715 spectropolarimeter (Jasco, Japan) over a spectral range of 200-350 nm with a scan speed of 50 nm min^{-1} and accumulation of three spectra for each measurement. All spectra were recorded at 25 °C. To study the influence of oxidation, 25 μM samples of reduced apo- or Zn_2γ-E_c-1 in 10 mM NaCl, 10 mM Tris-HCl, pH 7.5, were mixed with 2 mM (final concentration) H_2O_2, and the progress of the reaction monitored with CD spectra over time.

Mass spectrometry

Preparation of completely and partially oxidized γ-E_c-1 for MS analysis

Completely oxidized γ-E_c-1 was prepared as described above by overnight oxidation of Zn_2γ-E_c-1 with 2 mM H_2O_2. After dialysis and digestion with trypsin (see below) MS-MS analysis was performed.

Partially oxidized Zn_1γ-E_c-1 was obtained by incubation of 20 μM Zn_2γ-E_c-1 in 10 mM ammonium acetate, pH 7.5, with 1.5 mM H_2O_2 and control of the oxidation state at certain time intervals, i.e. 15, 50, and 120 min. The respective amount of reduced Cys residues was determined with the 2-PDS assay and the amount of remaining coordinated Zn(II) ions was measured with F-AAS after removal of loosely bound or released Zn(II) ions with Chelex® 100 resin. Two sample aliquots from each time point, one of them after modification with iodoacetamide and trypsin digestion (see below), were subjected to MS-MS analysis (see below).

Modification with iodoacetamide

20 μL of a 20 μM γ-E_c-1 solution were mixed with a 10-fold molar excess of iodoacetamide and incubated for 40 min in the dark. The reaction was stopped by freezing in liquid nitrogen. The non-reacted iodoacetamide was removed by C_{18} ZipTip (Millipore, Billerica, MA, USA) directly prior to MS measurements.

Trypsin digest

0.1 μg trypsin in 20 μL Tris-HCl, pH 5, was added to 10 μL of the respective protein solution (total amount 0.5 μg) in 10 mM ammonium acetate buffer, pH 7.5, and digestion was performed at rt for 90 min. The conditions, especially the low pH and temperature, were chosen to avoid scrambling of the disulfide bonds formed after initial oxidation of the protein. The resulting peptide digest mixture was desalted using a C_{18} ZipTip and spotted onto the MALDI target (MTP 384 target polished steel TF, Bruker Daltonics, Bremen, Germany) with 1:10 HPBA/CHCA in 50:50:0.1 ACN/H_2O/TFA (5 μg/ μL) for subsequent MALDI-TOF/TOF measurements.

MALDI-TOF/TOF measurement

MALDI measurements of trypsin digested samples were performed on an ultrafleXtreme MALDI-TOF/TOF mass spectrometer equipped with a smartbeam laser (Bruker Daltonics). The measurement parameters were programmed in flexControl (Version 3.4): laser frequency of 1000 Hz in the positive reflectron mode with acquisition ranging from 700 to 4000 Da. Final spectra consisted of 1000-3000 shots per analysis. MS and MS/MS data of ions of interest were acquired manually. The mass spectrometer was calibrated in MS mode for every new digest; in the MS/MS mode, the precursor ion was used as the reference mass in the individual analysis.

In order to prevent disulfide-bond reduction with CHCA during ionization, a 1:10 mixture of HBPA/CHCA was used; HBPA protects disulfides from reduction by being reduced preferentially.[60] Peptide fragments that are connected by disulfide bridges were identified using a high energy fragmentation technique. For this, MS/MS data were acquired using MALDI LIFT TOF/TOF mass spectrometry in the positive ion mode. The fragmentation was induced by the smartbeam laser without the further use of collision gas. Precursor ions were then accelerated and selected in the timed ion gate. In the LIFT cell the fragment ions were further accelerated and the MS/MS data recorded.

Electrospray-ionization mass spectrometry

Samples of Zn_2- or apo- (reduced or oxidized) γ-E_c-1 in 10 mM NH_4HCO_3, pH 7.0, or 2 mM HCl depending on downstream experiments were injected directly or with a prior

acidification step into an Synapt G2 quadrupole time-of-flight spectrometer (Waters, UK). For analysis at neutral pH 10 mM NH_4Ac in 50% MeOH, pH 7.5, was used, at acidic pH 50% ACN and 0.2% formic acid, pH 2–3, (final concentrations) were added. Scans were accumulated and further processed with the software MassLynx 3.5 (Micromass). Deconvolution of MS data was done by applying the maximum entropy algorithm of the MassLynx tool MaxEnt1. Electrospray parameters were capillary voltage 2.6 V, cone voltage 50 V, and source temperature 80 °C.

REFERENCES

1. Cobbett, C.; Goldsbrough, P. Annu Rev Plant Biol 2002, 53, 159-182.
2. Jacob, C.; Maret, W.; Vallee, B. L. Proc Natl Acad Sci USA 1998, 95, 3489-3494.
3. Suzuki, K. T.; Someya, A.; Komada, Y.; Ogra, Y. J Inorg Biochem 2002, 88, 173-182.
4. Vašák, M.; Kägi, J. H. R.; Holmquist, B.; Vallee, B. L. Biochemistry 1981, 20, 6659-6664.
5. Anderson, R. S.; Patel, K. M.; Roesijadi, G. Dev Comp Immunol 1999, 23, 443-449.
6. Abel, J.; de Ruiter, N. Toxicol Lett 1989, 47, 191-196.
7. Gupta, V.; Carroll, K. S. Biochim Biophys Acta 2014, 1840, 847-875.
8. Lo Conte, M.; Carroll, K. S. In Oxidative stress and redox regulation; Jakob, U., Reichmann, D., Eds.; Springer: New York, 2013, pp 1-42.
9. Yang, Y.; Maret, W.; Vallee, B. L. Proc Natl Acad Sci USA 2001, 98, 5556-5559.
10. Maret, W. J Biol Inorg Chem 2011, 16, 1079-1086.
11. Cano-Gauci, D. F.; Sarkar, B. FEBS Lett 1996, 386, 1-4.
12. Davis, S. R.; Cousins, R. J. J Nutr 2000, 130, 1085-1088.
13. Chandhok, G.; Schmitt, N.; Sauer, V.; Aggarwal, A.; Bhatt, M.; Schmidt, H. H. J. PLoS ONE 2014, 9, e98809.
14. Hassinen, V. H.; Tervahauta, A. I.; Schat, H.; Karenlampi, S. O. Plant Biology 2011, 13, 225-232.
15. Haase, H.; Maret, W. Anal Biochem 2004, 333, 19-26.
16. Freisinger, E. Chimia 2010, 64, 217-224.
17. Vašák, M.; Meloni, G. J Biol Inorg Chem 2011, 16, 1067-1078.
18. Wüthrich, K. NMR of proteins and nucleic acids; Wiley-Interscience: New York, 1986.
19. Schicht, O.; Freisinger, E. Inorg Chim Acta 2009, 362, 714-724.
20. Summers, K. L.; Mahrok, A. K.; Dryden, M. D. M.; Stillman, M. J. Biochem Bioph Res Co 2012, 425, 485-492.
21. Zangger, K.; Öz, G.; Haslinger, E.; Kunert, O.; Armitage, I. M. FASEB J 2001, 15, 1303-1305.
22. Zangger, K.; Shen, G.; Öz, G.; Otvos, J. D.; Armitage, I. M. Biochem J 2001, 359, 353-360.
23. Isani, G.; Andreani, G.; Kindt, M.; Carpenè, E. Cell Mol Biol 2000, 46, 311-330.
24. Mackay, E. A.; Overnell, J.; Dunbar, B.; Davidson, I.; Hunziker, P. E.; Kägi, J. H. R.; Fothergill, J. E. Eur J Biochem 1993, 218, 183-194.
25. Kawashima, I.; Kennedy, T. D.; Chino, M.; Lane, B. G. Eur J Biochem 1992, 209, 971-976.
26. Loebus, J.; Peroza, E. A.; Blüthgen, N.; Fox, T.; Meyer-Klaucke, W.; Zerbe, O.; Freisinger, E. J Biol Inorg Chem 2011, 16, 683-694.
27. Peroza, E. A.; Freisinger, E. J Biol Inorg Chem 2007, 12, 377-391.
28. Peroza, E. A.; Schmucki, R.; Güntert, P.; Freisinger, E.; Zerbe, O. J Mol Biol 2009, 387, 207-218.

29. Jiménez, I.; Gotteland, M.; Zarzuelo, A.; Uauy, R.; Speisky, H. Toxicology 1997, 120, 37-46.
30. Savas, M. M.; Shaw, C. F.; Petering, D. H. J Inorg Biochem 1993, 52, 235-249.
31. Zhang, S.; Li, J.; Wang, C. C.; Tsou, C. L. FEBS Lett 1999, 462, 383-386.
32. Peroza, E. A.; Cabral, A.; Wan, X.; Freisinger, E. Metallomics 2013, 5, 1204-1214.
33. Hoshi, T.; Heinemann, S. H. J Physiol 2001, 531, 1-11.
34. Jocelyn, P. C. Eur J Biochem 1967, 2, 327-331.
35. Kimura, R. H.; Tran, A. T.; Camarero, J. A. Angew Chem Int Ed 2006, 45, 973-976.
36. Aboye, T. L.; Clark, R. J.; Burman, R.; Roig, M. B.; Craik, D. J.; Goransson, U. Antioxid Redox Sign 2011, 14, 77-86.
37. Quesada, A. R.; Byrnes, R. W.; Krezoski, S. O.; Petering, D. H. Arch Biochem Biophys 1996, 334, 241-250.
38. Aravindakumar, C. T.; Ceulemans, J.; De Ley, M. Biochem J 1999, 344, 253-258.
39. Edelhoch, H. Biochemistry 1967, 6, 1948-1954.
40. Claiborne, A.; Yeh, J. I.; Mallett, T. C.; Luba, J.; Crane, E. J.; Charrier, V.; Parsonage, D. Biochemistry 1999, 38, 15407-15416.
41. Rehder, D. S.; Borges, C. R. Biochemistry 2010, 49, 7748-7755.
42. Maret, W.; Vallee, B. L. Proc Natl Acad Sci USA 1998, 95, 3478-3482.
43. Guggenheim, E. A. Phil Mag 1926, 2, 538-543.
44. Kelly, S. M.; Jess, T. J.; Price, N. C. Biochim Biophys Acta 2005, 1751, 119-139.
45. Freisinger, E.; Vašák, M. Met Ions Life Sci 2013, 11, 339-371.
46. Meloni, G.; Sonois, V.; Delaine, T.; Guilloreau, L.; Gillet, A.; Teissie, J.; Faller, P.; Vasak, M. Nature Chem Biol 2008, 4, 366-372.
47. Biteau, B.; Labarre, J.; Toledano, M. B. Nature 2003, 425, 980-984.
48. Rhee, S. G.; Jeong, W.; Chang, T. S.; Woo, H. A. Kidney Int 2007, 72, S3-S8.
49. Woo, H. A.; Jeong, W. J.; Chang, T. S.; Park, K. J.; Park, S. J.; Yang, J. S.; Rhee, S. G. J Biol Chem 2005, 280, 3125-3128.
50. Yang, K. S.; Kang, S. W.; Woo, H. A.; Hwang, S. C.; Chae, H. Z.; Kim, K.; Rhee, S. G. J Biol Chem 2002, 277, 38029-38036.
51. Rellan-Alvarez, R.; Hernandez, L. E.; Abadia, J.; Alvarez-Fernandez, A. Anal Biochem 2006, 356, 254-264.
52. Craik, D. J.; Daly, N. L.; Bond, T.; Waine, C. J Mol Biol 1999, 294, 1327-1336.
53. Felizmenio-Quimio, M. E.; Daly, N. L.; Craik, D. J. J Biol Chem 2001, 276, 22875-22882.
54. Wan, X.; Freisinger, E. Metallomics 2009, 1, 489-500.
55. Freisinger, E. Inorg Chim Acta 2007, 360, 369-380.

56. Roschitzki, B.; Vašák, M. J Biol Inorg Chem 2002, 7, 611-616.
57. Hudson, D. A.; Gannon, S. A.; Thorpe, C. Free Radical Bio Med 2015, 80, 171-182.
58. Pedersen, A. O.; Jacobsen, J. Eur J Biochem 1980, 106, 291-295.
59. Scopes, R. K. Anal Biochem 1974, 59, 277-282.
60. Huwiler, K. G.; Mosher, D. F.; Vestling, M. M. J Biomol Tech 2003, 14, 289-297.

FIGURE LEGENDS

FIGURE 1 Scheme of proposed interchange mechanisms between different MT forms found in the plant cell (abbreviations used: ROS/RNS, reactive oxygen/nitrogen species; Grx, glutaredoxin; GSR, glutathione-disulfide reductase; Trx, thioredoxin; TR, thioredoxin reductase). A metal chelator can be any compound, e.g. apo-proteins or small molecules, with a metal ion binding affinity similar to or higher than the one of the respective MT.

FIGURE 2 Schematic presentation of different conditions used for the oxidation of apo- and $Zn_2\gamma$-E_c-1 and the resulting species.

FIGURE 3 Oxidation of 10 μM $Zn_2\gamma$-E_c-1 with 2 mM H_2O_2. (**A**) Time dependent evolution of absorption spectra. The absorption range 255-310 nm is marked with a box and enlarged in (**B**). (**B**) Enlarged absorption range 255-310 nm, after subtraction of the initial $Zn_2\gamma$-E_c-1 spectrum from all other spectra, showing the evolution of a broad absorption band originating from disulfide bridge formation. (**C**) Plot of time dependent absorptivity changes at 230 (black squares, right axis) and 280 nm (grey open squares, left axis). The decrease in absorption at 230 nm results from Zn(II) release from the metal-thiolate cluster, the appearance of the broad absorption band centered at 280 nm is indicative for disulfide bridge formation. Below the graph the hypothetical species present at 50, 75, and 100% Zn(II) release are given (see text for discussion).

FIGURE 4 Oxidation of 10 μM $Zn_2\gamma$-E_c-1 with 2 mM H_2O_2 in presence of 100 μM zincon leading to formation of the Zn(II)-zincon complex. (**A**) Plot of the Zn(II)-zincon complex absorption at 620 nm against incubation time. (**B**) Plot of $\ln((A_{start}-A_t)/(A_{start}-A_{end}))$ against time (black dots) for the determination of the first-order rate constants (k) of Zn(II) release from $Zn_2\gamma E_c$-1 with equation 1. The linear fits for the different time ranges are depicted as dashed lines and result in the following values: 0-50 min (= 25% Zn^{II} release), $k_1 = (6.63 \pm 0.97) \cdot 10^{-4}$ s^{-1}; 50-110 min (= 50% Zn^{II} release), $k_2 = (1.88 \pm 0.11) \cdot 10^{-4}$ s^{-1}; 110-190 min (= 75% Zn^{II} release), $k_3 = (0.78 \pm 0.04) \cdot 10^{-4}$ s^{-1}; 190-380 min (= 100% Zn^{II} release), $k_4 = (0.22 \pm 0.02) \cdot 10^{-4}$ s^{-1}; 0-380 min, $k_{av} = (0.97 \pm 0.14) \cdot 10^{-4}$ s^{-1} .

FIGURE 5 CD spectra taken at different time points (see legend) during the oxidation of 25 μM solutions of Zn_2γ-E_c-1 (black) or reduced apo-γ-E_c-1 (grey) with 2 mM H_2O_2. Ellipticity values below approximately 210 nm (grey box) are not reliable due to saturation of the CD detector at the protein concentration used.

FIGURE 6 (**A**) Amino acid sequence alignment of the γ-E_c-1 domain with the sequence of the cyclic MCoTI-II protein (PDB ID: 1IB9) revealing a sequence identity of 32 % (marked with *) and a sequence similarity of 44 % (marked with .; Clustal Omega server, http://www.ebi.ac.uk/Tools/msa/clustalo/). The disulfide bridge connectivities determined for MCoTI-II are indicated above the sequence.[53] (**B**) Solution structure of Zn_2γE_c-1 (2L61) obtained by NMR spectroscopy with cysteine sulfur atoms depicted as white balls and Zn(II) ions as grey spheres. The disulfide connectivities predicted by mass spectrometry are indicated by dashed lines. (**C**) Amino acid sequence of γ-E_c-1 with proposed disulfide connectivities based on the MS data.

FIGURE 7 Species observed in the MS data during the oxidation of Zn_2γ-E_c-1 with H_2O_2. Zn(II) ions are shown as green spheres, reduced Cys residues as black and oxidized Cys as orange circles, disulfide bridges are depicted with an orange and Zn-S bonds with a grey line. The predicted position of the remaining Zn(II) ion in the partially oxidized Zn_1γ-E_c-1 form is indicated by a green sphere and a "?". The backbone of the peptide fragments observed with MS is colored black, while the rest of the backbone is grey.

FIGURE 8 (**A**) Amino acid sequence of the γ-E_c-1 domain with potential proteinase K cleavage sites indicated. Size exclusion chromatograms of 40 μM solutions of (**B**) Zn_2-, (**C**) reduced, and (**D**) oxidized apo-γ-E_c-1 prior (black dashed lines) and after (black solid lines) incubation with proteinase K in a molar ratio of 5:1. The chromatogram of a control solution containing only proteinase K is depicted as a grey dotted line in each part. The peptide fragments observed in the MS data of the main peaks marked with * are given below each chromatogram. For details on MS data assignment see Figure S23, Supporting Information. In addition, oxidized γ-E_c-1 was

also incubated with a 5-times higher amount of proteinase K (1:1 molar ratio, black thin line in (D)), however, the peak corresponding to full length γ-E_c-1 is still detected.

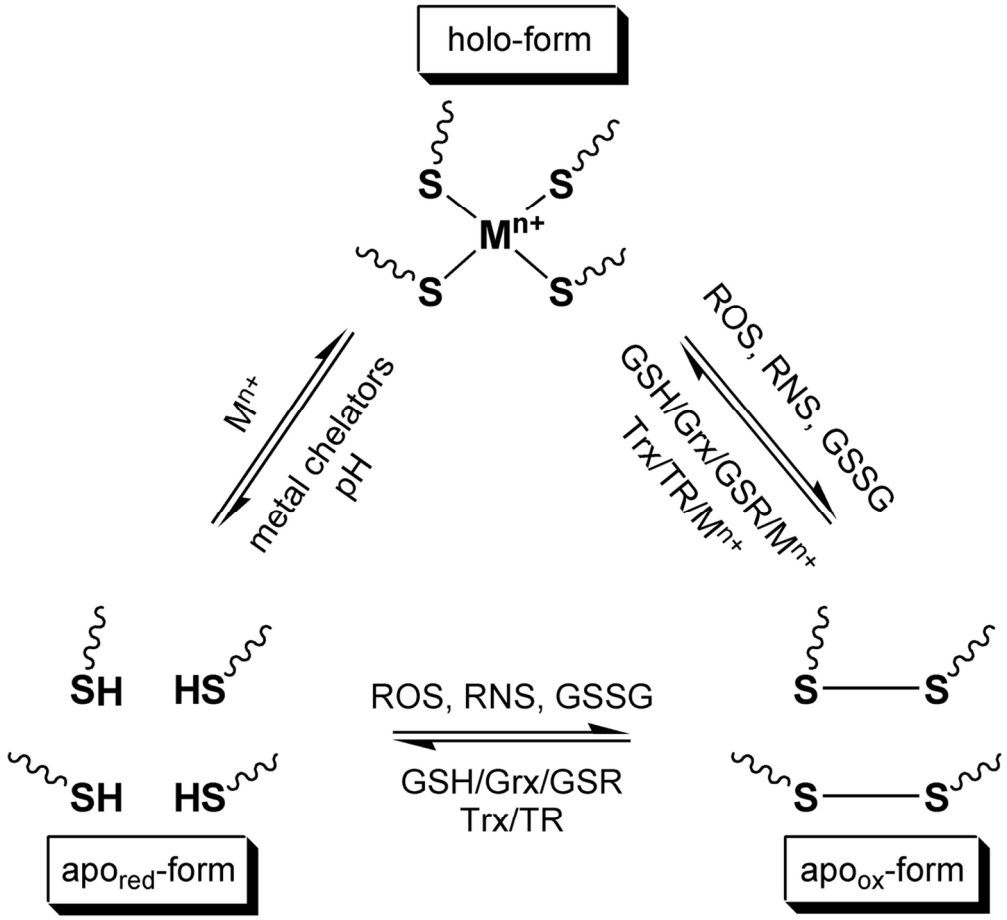

Figure 1. Scheme of proposed interchange mechanisms between different MT forms found in the plant cell (abbreviations used: ROS/RNS, reactive oxygen/nitrogen species; Grx, glutaredoxin; GSR, glutathione-disulfide reductase; Trx, thioredoxin; TR, thioredoxin reductase). A metal chelator can be any compound, e.g. apo-proteins or small molecules, with a metal ion binding affinity similar to or higher than the one of the respective MT.
112x102mm (300 x 300 DPI)

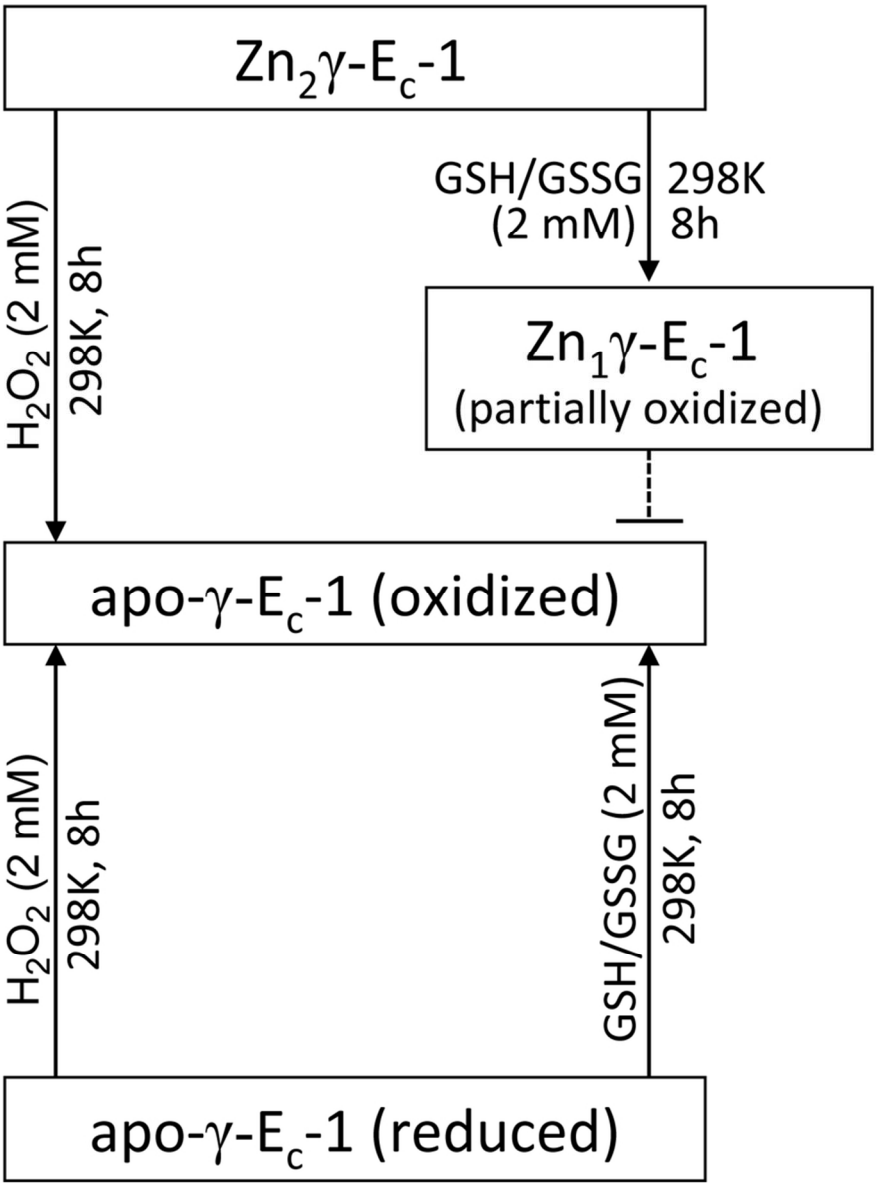

Figure 2. Schematic presentation of different conditions used for the oxidation of apo- and $Zn_2\gamma$-E_c-1 and the resulting species.
77x103mm (300 x 300 DPI)

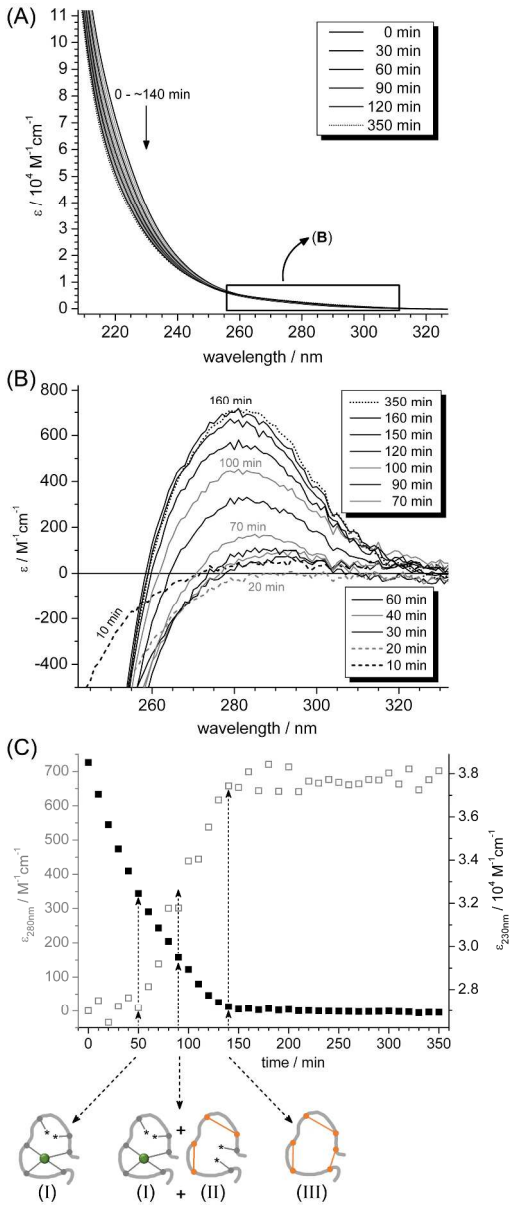

Figure 3. Oxidation of 10 μM $Zn_2\gamma$-E_c-1 with 2 mM H_2O_2. (A) Time dependent evolution of absorption spectra. The absorption range 255-310 nm is marked with a box and enlarged in (B). (B) Enlarged absorption range 255-310 nm, after subtraction of the initial $Zn_2\gamma$-E_c-1 spectrum from all other spectra, showing the evolution of a broad absorption band originating from disulfide bridge formation. (C) Plot of time dependent absorptivity changes at 230 (black squares, right axis) and 280 nm (grey open squares, left axis). The decrease in absorption at 230 nm results from Zn(II) release from the metal-thiolate cluster, the appearance of the broad absorption band centered at 280 nm is indicative for disulfide bridge formation. Below the graph the hypothetical species present at 50, 75, and 100% Zn(II) release are given (see text for discussion).
247x580mm (300 x 300 DPI)

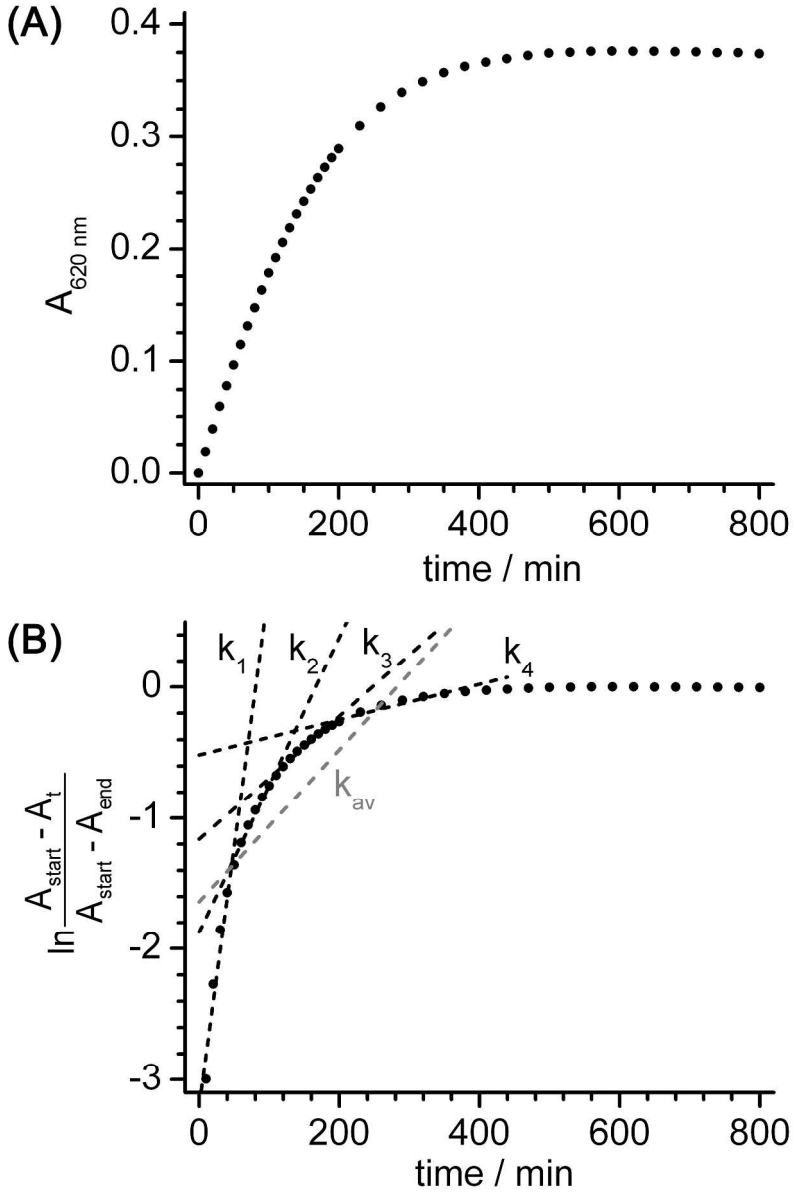

Figure 4. Oxidation of 10 μM $Zn_2\gamma$-E_c-1 with 2 mM H_2O_2 in presence of 100 μM zincon leading to formation of the Zn(II)-zincon complex. (A) Plot of the Zn(II)-zincon complex absorption at 620 nm against incubation time. (B) Plot of $\ln((A_{start}-A_t)/(A_{start}-A_{end}))$ against time (black dots) for the determination of the first-order rate constants (k) of Zn(II) release from $Zn_2\gamma E_c$-1 with equation 1. The linear fits for the different time ranges are depicted as dashed lines and result in the following values: 0-50 min (= 25% Zn(II) release), k_1 = (6.63 ± 0.97) • 10^{-4} s^{-1}; 50-110 min (= 50% Zn(II) release), k_2 = (1.88 ± 0.11) • 10^{-4} s^{-1}; 110-190 min (= 75% Zn(II) release), k_3 = (0.78 ± 0.04) • 10^{-4} s^{-1}; 190-380 min (= 100% Zn(II) release), k_4 = (0.22 ± 0.02) • 10^{-4} s^{-1}; 0-380 min, k_{av} = (0.97 ± 0.14) • 10^{-4} s^{-1} .
255x385mm (300 x 300 DPI)

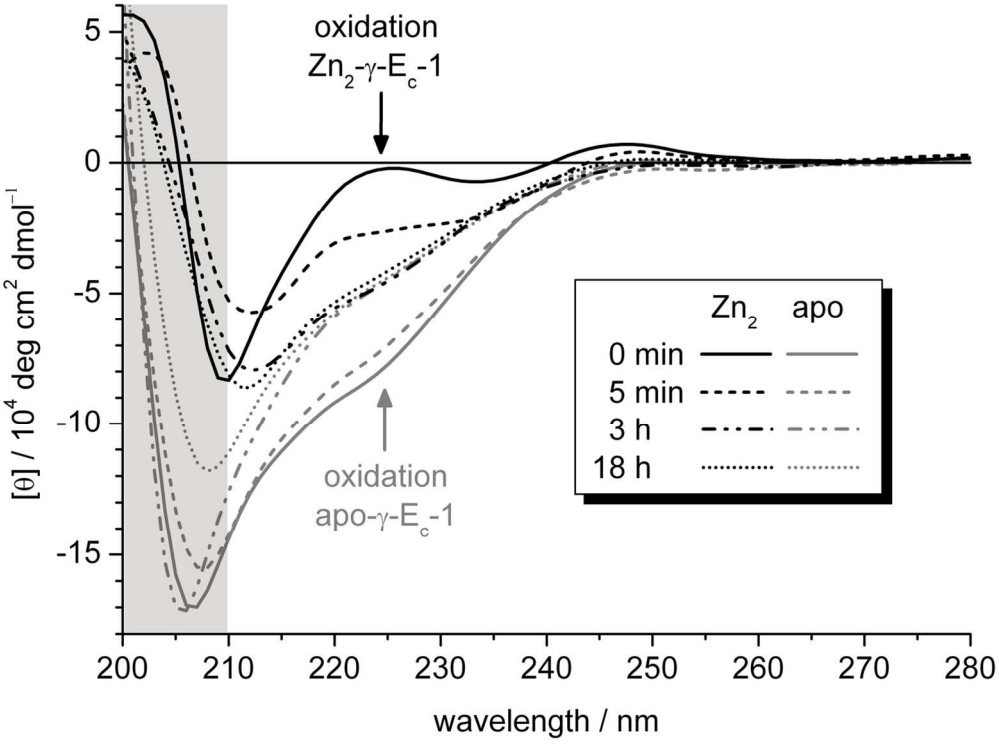

Figure 5. CD spectra taken at different time points (see legend) during the oxidation of 25 μM solutions of Zn_2γ-E_c-1 (black) or reduced apo-γ-E_c-1 (grey) with 2 mM H_2O_2. Ellipticity values below approximately 210 nm (grey box) are not reliable due to saturation of the CD detector at the protein concentration used.
126x93mm (300 x 300 DPI)

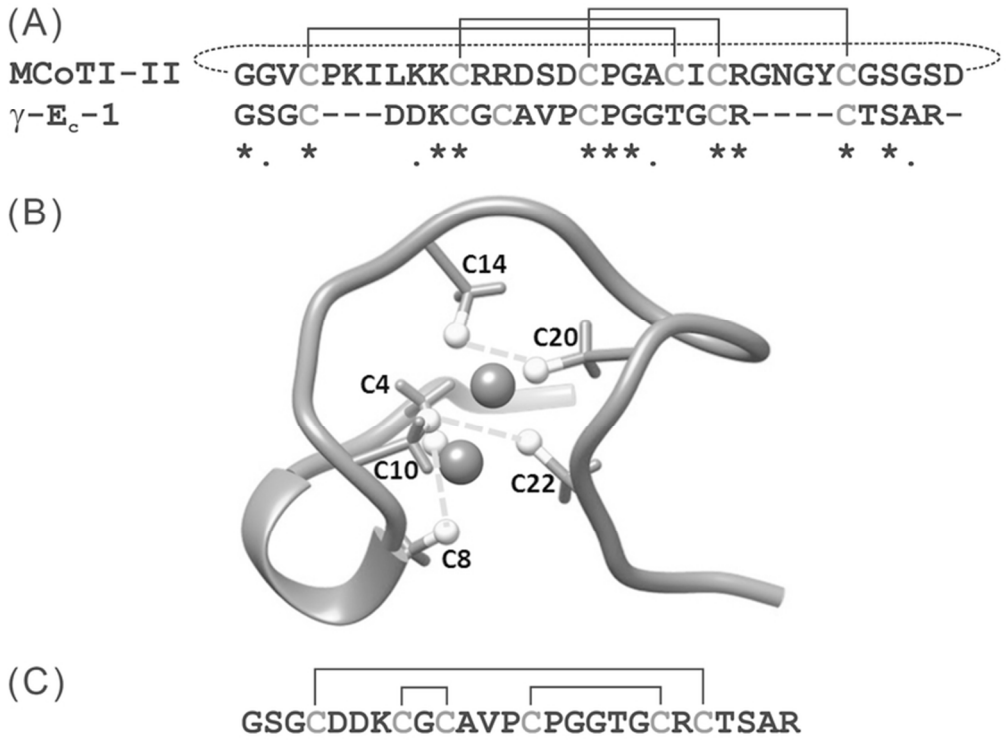

Figure 6. (A) Amino acid sequence alignment of the γ-E_c-1 domain with the sequence of the cyclic MCoTI-II protein (PDB ID: 1IB9) revealing a sequence identity of 32 % (marked with *) and a sequence similarity of 44 % (marked with .; Clustal Omega server, http://www.ebi.ac.uk/Tools/msa/clustalo/). The disulfide bridge connectivities determined for MCoTI-II are indicated above the sequence.[53] (B) Solution structure of Zn_2γE_c-1 (2L61) obtained by NMR spectroscopy with cysteine sulfur atoms depicted as white balls and Zn(II) ions as grey spheres. The disulfide connectivities predicted by mass spectrometry are indicated by dashed lines. (C) Amino acid sequence of γ-E_c-1 with proposed disulfide connectivities based on the MS data.
69x51mm (300 x 300 DPI)

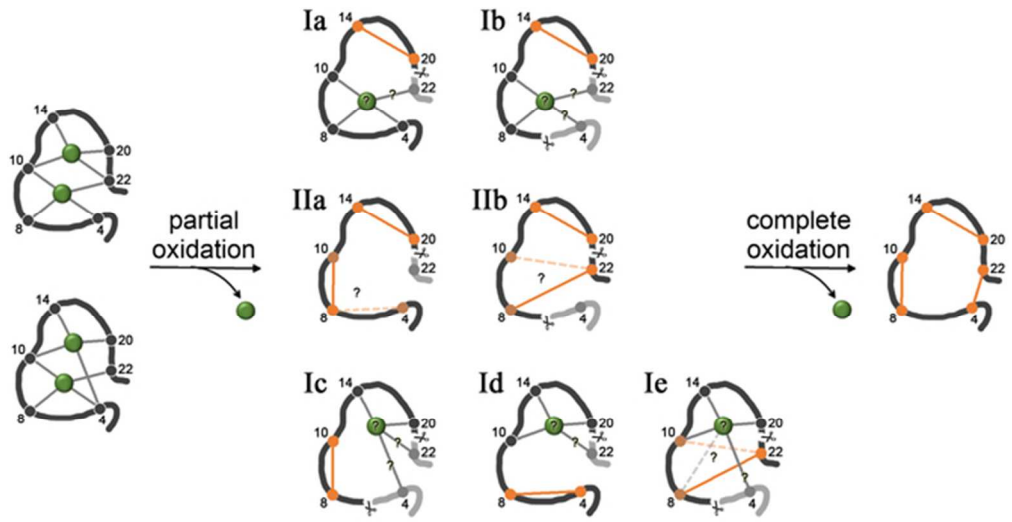

Figure 7. Species observed in the MS data during the oxidation of $Zn_2\gamma$-E_c-1 with H_2O_2. Zn(II) ions are shown as green spheres, reduced Cys residues as black and oxidized Cys as orange circles, disulfide bridges are depicted with an orange and Zn-S bonds with a grey line. The predicted position of the remaining Zn(II) ion in the partially oxidized $Zn_1\gamma$-E_c-1 form is indicated by a green sphere and a "?". The backbone of the peptide fragments observed with MS is colored black, while the rest of the backbone is grey.
56x28mm (300 x 300 DPI)

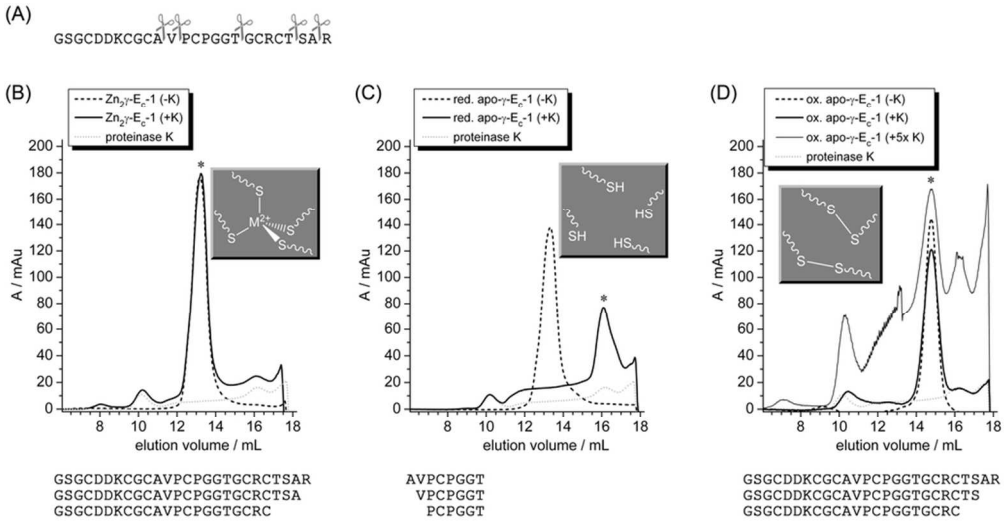

Figure 8. (A) Amino acid sequence of the γ-E_c-1 domain with potential proteinase K cleavage sites indicated. Size exclusion chromatograms of 40 µM solutions of (B) Zn_2-, (C) reduced, and (D) oxidized apo-γ-E_c-1 prior (black dashed lines) and after (black solid lines) incubation with proteinase K in a molar ratio of 5:1. The chromatogram of a control solution containing only proteinase K is depicted as a grey dotted line in each part. The peptide fragments observed in the MS data of the main peaks marked with * are given below each chromatogram. For details on MS data assignment see Figure S23, Supporting Information. In addition, oxidized γ-E_c-1 was also incubated with a 5-times higher amount of proteinase K (1:1 molar ratio, black thin line in (D)), however, the peak corresponding to full length γ-E_c-1 is still detected.
87x45mm (300 x 300 DPI)